Eur. Phys. J. Special Topics **228**, 2381–2389 (2019)

https://doi.org/10.1140/epjst/e2019-900077-7

THE EUROPEAN PHYSICAL JOURNAL SPECIAL TOPICS

Regular Article

Dynamics of functional connectivity in multilayer cortical brain network during sensory information processing

Nikita S. Frolov[1], Vladimir A. Maksimenko[1], Marina V. Khramova[2], Alexander N. Pisarchik[1,3], and Alexander E. Hramov[1,a]

[1] Neuroscience and Cognitive Technology Laboratory, Innopolis University, Innopolis, The Republic of Tatarstan, Russia
[2] Faculty of Computer Science, Saratov State University, Saratov, Russia
[3] Center for Biomedical Technology, Technical University of Madrid, Campus Montegancedo, Spain

Received 30 April 2019 / Received in final form 20 June 2019
Published online 28 October 2019

Abstract. Topology of a functional brain multilayer network is dynamically adjusted to provide optimal performance during accomplishing cognitive tasks, including sensory information processing. Functional connectivity between brain regions is achieved in terms of correlation or synchronization inference in recorded signals of neuronal activity. The promising approach for studying cortical network structure implies considering functional interactions in different frequency bands on the different layers of multilayer network model. Links between these layers can be restored based on cross-frequency couplings. While the topology of functional connectivity within each layer can be effectively restored from registered neurophysiological signals, mechanisms underlying coupling between different layers remain poorly understood. Here we consider evolution of the cortical network topology in alpha and beta frequency bands during visual stimuli processing. For each frequency band the functional connectivity between different brain regions is estimated by comparing Fourier spectra of EEG signals. The obtained functional topologies are considered as the layers of two-layer network. In the framework of a multilayer model we analyze evolution of functional network topology on both layers and reveal features of intralayer interaction underlying visual information processing in the brain.

1 Introduction

Topology of a cortical brain network is dynamically adjusted to provide optimal performance during accomplishing cognitive tasks, including sensory information processing [1–4]. For instance, a small amount of visual information which can effortlessly be processed activates neural populations in occipital and parietal areas. Conversely, a visual task which requires sustained attention to process a large amount of

[a] e-mail: a.hramov@innopolis.ru

sensory information involves a set of long-distance connections between parietal and frontal areas coordinating the activity of these distant brain regions [5,6]. According to the recent review [7], mechanisms of neural interactions within the cortical network underlying cognitive performance are poorly understood.

The cortical brain network is usually studied by topology reconstruction from a set of multichannel recordings of neuronal activity (fMRI, fNIRS, EEG, MEG, etc.). Here, functional connectivity between the brain regions is achieved in terms of correlation or synchronization inference in recorded signals. There are several techniques which are used to estimate a functional connectivity. In particular, functional connectivity can be measured via Granger causality [8], nonlinear correlations [9] and entropy transfer methods [10].

According to recent study [11], neural interactions between the brain regions are subserved by coherence of registered signals of brain activity. Therefore, the coupling strength between brain regions can be estimated by measuring coherence of the corresponding neurophysiological signals. One of the effective approaches to evaluate coherence in a pair of signals is the wavelet bicoherence (WBC). WBC measures the amount of phase coupling in the time interval that occurs between wavelet components of considered signals. WBC is a powerful tool for biological signal analysis [4,12–14].

As WBC implies, the coherence between signals can be measured in different frequency bands simultaneously. This is of a particular interest for analysis of the cortical network, since the neural ensembles interact through different bands [11,15]. In particular, recent work [14,16] reports that neuronal populations belonging to the remote brain regions interact in different frequency bands with different degrees of intensity. Authors reconstructed topology of the brain links in different frequency bands and found different structures associated with normal brain state and pathological behavior. During sensory processing tasks the neural populations in visual cortex are shown to interact in 8–30 Hz and 50–70 Hz [8,17]. Moreover, according to recent work [18], visual sensory processing engages neuronal interactions in 8–12 Hz (alpha-band) and 15–30 Hz (beta-band) with different topological properties.

Thus, considering the neural interactions in the different frequency bands is a promising approach for understanding functions of the cortical brain network. In the framework of this approach, interactions between the neuronal populations can be described in terms of multilayer network, where each layer represents the coupling topology in a particular frequency band. Whereas the topology of neural interactions in each layer can be effectively restored from registered neurophysiological electroencephalographical (EEG) signals, mechanisms underlying coupling strength between different layers remain poorly understood [4,19].

According to Canolty et al. [20], there is a robust coupling between the high- and low-frequency bands of electrical activity in the human brain. In particular, the phase of theta-rhythm (4–8 Hz) modulates power of gamma-rhythm (80–150 Hz) oscillations on the electrocorticograms (ECoG). Furthermore, different behavioral tasks evoke distinct patterns of theta/gamma band couplings across the cortex. For instance, continuous mental arithmetic tasks demanding the retention and summation of items in the working memory enhanced the cross-frequency phase synchrony among alpha, beta-, and gamma-oscillations [21]. Therefore, along with the neural interactions in a particular frequency bands, analysis of interlayer (cross-frequency) coupling is of great interest and remains an actively studied topic in physics and neuroscience [22,23].

Having summarized, the promising approach for studying cortical network structure implies considering neural interactions in different frequency bands on the different layers of multilayer network model. Links between these layers can be restored based on cross-frequency coupling. Experimental results evidence that brain

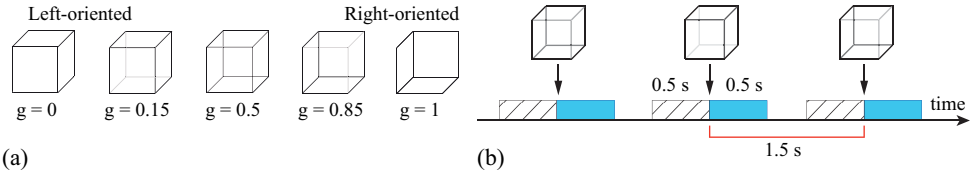

Fig. 1. Illustration of bistable visual stimuli and experimental procedure. (a) Images of Necker cube depending on edges contrast g. (b) Subsets of *easy* and *hard* visual stimuli used during the experiment. (c) Sketch illustrating experimental procedure – visual stimuli was presented at time moments represented by arrows and demonstrated for about 0.5 s. Time interval between visual stimuli presentations was about 1.5 s.

functioning affects both within-frequency (inter-layer) synchrony in different frequency bands and the cross-frequency (intra-layer) phase synchrony between them. With this in mind we consider evolution of the cortical network topology in alpha and beta frequency bands during visual sensory processing. For each frequency band the coupling strength between different brain regions was estimated by comparing Fourier spectra of the corresponding EEG signals. As it has been shown [14] this approach enables restoring functional connectivity based on the degree of phase synchronization between EEG signals. Having analyzed the evolution of layer's topology in time, we reveal the typical scenarios of cortical network reconfiguration during visual stimuli processing.

2 Methods

2.1 Experimental procedure and participants

Ten healthy subjects from a research team of Innopolis University, males and females, between the ages of 20 and 30 with normal or corrected-to-normal visual acuity participated in the experiments. All participants provided informed written consent before participating in the experiment. The experimental studies were performed in accordance with the Declaration of Helsinki and approved by the local research ethics committee of Innopolis University.

During the experiment the participants were asked to interpret a bistable visual stimulus demonstrated on the screen in front of them. The Necker cube [24–27], which is presented as a 2D image of cube with transparent faces and visible edges, was used as a bistable visual stimulus.

A subject without any perception abnormalities sees the Necker cube as a 3D-object due to the specific position of the cube's edges. Bistability in perception consists in the interpretation of this 3D-object as to be either left-oriented or right-oriented cube depending on the contrast of different inner edges of the cube. The contrast $g \in [0, 1]$ of the three inner lines centered in the left lower corner is used as a control parameter. The contrast of the other three inner lines centered in the right upper corner was set to $(1 - g)$. The values $g = 1$ and $g = 0$ correspond, respectively, to 0 (black) and 255 (white) pixels' luminance of the inner lines. Therefore, we can define a contrast parameter as $g = y/255$, where y is the brightness level of the inner lines using the 8-bit gray-scale palette. The examples of Necker-cube images with different values of g–parameter are shown in Figure 1a.

The whole set of Necker cubes included images with eight different values of control parameter: $g = (0.15, 0.25, 0.4, 0.45, 0.55, 0.60, 0.75, 0.85)$. Each image was presented 20 times, i.e. 160 times for all set. In order to capture the first impression of the participant each bistable image was demonstrated during 0.5–0.7 s with an interval

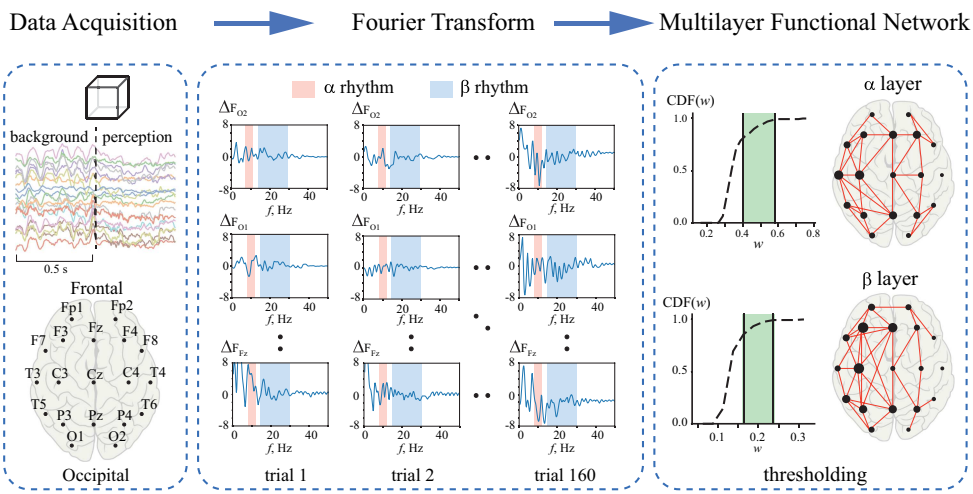

Fig. 2. Schematic representation of the algorithm for reconstructing multilayer functional network from experimental EEG data.

of about 1.5 s between demonstrations [28] (Fig. 1b). The stimuli were demonstrated on a 24″ LCD monitor with a spatial resolution of 1920 × 1080 pixels and a 60 Hz refresh rate. Each Necker cube image with black and grey ribs was displayed in the middle of a computer screen on a white background. The subjects were sitting at a 70–80 cm distance from the monitor with an approximately 0.25-rad visual angle.

EEG data were acquired with 19 noninvasive electrodes located according to "10-20" electrode layout. To register EEG data, cup adhesive Ag/AgCl electrodes were placed on the scalp with the help of "Tien–20" paste. The ground electrode was located above the forehead, while referents were attached to mastoids. For filtering EEG signals, a band-pass filter with cut-off points at 0.016 Hz (HP) and 70 Hz (LP) and a 50 Hz Notch filter were used. For EEG signal amplification and analog-to-digital conversion, the electroencephalograph "Encephalan–EEGR–19/26" ("Medikom-MTD", Taganrog, Russian Federation) with multiple EEG channels was used.

2.2 Multilayer network reconstruction

Functional connectivity between the distinct neuronal populations was reconstructed from the recorded multichannel EEG signals in alpha (8–14 Hz) and beta (15–30 Hz) frequency bands. The functional relation between a pair of neuronal populations was assessed in terms of phase synchronization between corresponding EEG signals. According to a recent work [14], phase synchronization between neural populations reflects a similarity between the features of their oscillatory activity in a frequency domain on short time scales. Thus, to reconstruct the functional connectivity between neuronal ensembles in alpha and beta frequency bands we compared the spectral components of their EEG signals belonging to these bands. A Schematic representation of network reconstruction algorithm is presented in Figure 2. It is implemented in three steps.

– EEG data were cut into a set of 1 second trials associated with visual stimuli presentation (Fig. 2a, upper panel). Then, $\mathbf{x}(t) = \{x_1(t), ...x_{N_{ch}}(t)\}^T$ was considered as a multivariate EEG trial that included background activity (0.5 s prior visual stimuli presentation as shown in Fig. 1b) and perception phase (0.5 s after visual

stimuli presentation as shown in Fig. 1b), N_{ch} is the number of considered EEG channels. The stimulus-related changes in frequency domain ΔF_i is defined for ith EEG channel as a difference between Fourier spectra calculated during the perception phase and background

$$\Delta F_i(f) = \frac{1}{\sqrt{2\pi}} \left[\int_{0}^{0.5\,\mathrm{s}} x_i(t) e^{-j2\pi f t} dt - \int_{-0.5\,\mathrm{s}}^{0} x_i(t) e^{-j2\pi f t} dt \right]. \tag{1}$$

In Figure 2b the obtained coefficients ΔF_i are arranged in the form of matrix where each row corresponds to EEG channel and each column to the single trial.

– The weighted functional links between ith and jth EEG channels in alpha and beta bands were reconstructed based on pair-wise distance between stimulus-related changes ΔF_i and ΔF_j,

$$w_{ij}^{\alpha} = \left[\sqrt{\int_{f=8\,\mathrm{Hz}}^{14\,\mathrm{Hz}} (\Delta F_i(f) - \Delta F_j(f))^2} \right]^{-1}, \tag{2}$$

$$w_{ij}^{\beta} = \left[\sqrt{\int_{f=15\,\mathrm{Hz}}^{30\,\mathrm{Hz}} (\Delta F_i(f) - \Delta F_j(f))^2} \right]^{-1}. \tag{3}$$

Obtained weights $w_{ij}^{\alpha,\beta}$ were averaged over all trials. As a result, reconstructed network represented a fully-connected weighted graph.

– To extract significant links in reconstructed network, we applied thresholding and constructed binary adjacency matrices W^{α} and W^{β} that contained only strong links belonging to the range between 80th and 99th percentiles of weight distribution CDF(w) (Fig. 2c, left panel). Thus, reconstructed network took the form of sparse unweighted two-layer network, where each layer reflected functional connectivity in alpha and beta frequency ranges (Fig. 2c, right panel).

Using the reconstructed two-layer network we have analyzed the dynamics of functional connectivity during sensory information processing. For this purpose the network reconstruction algorithm was applied in a 0.5 s floating window. The current position of the window was defined by τ which corresponded to the right border of the window. As a result, equation (1) was rewritten in window-like form

$$\Delta F_i(f,\tau) = \frac{1}{\sqrt{2\pi}} \left[\int_{\tau-0.5\,\mathrm{s}}^{\tau} x_i(t) e^{-j2\pi f t}\, dt - \int_{-0.5\,\mathrm{s}}^{0} x_i(t) e^{-j2\pi f t}\, dt \right], \tag{4}$$

where the second term in the brackets remained unchanged and defined EEG spectral properties during the background and the first term reflected spectral properties in a floating window during perception.

To characterize a collective behavior in both alpha and beta layers of considered two-layer network we have introduced a measure of topological similarity σ as follows:

$$\sigma = \frac{1}{N_{ch}^2} \sum_{i=1}^{N_{ch}} \sum_{j=1}^{N_{ch}} W_{i,j}^{\alpha} \circ W_{i,j}^{\beta}, \tag{5}$$

where $\circ$ stand for the element-wise multiplication. In this definition $\sigma = 0$ indicated no topological similarity (identity) between network layers, whereas $\sigma = 1$ evidenced complete similarity of layers' topology.

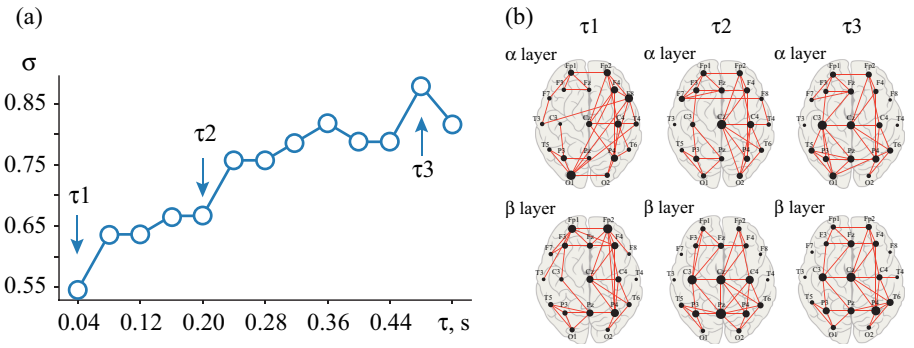

Fig. 3. Typical dynamics of two-layer network topology during the visual task performance captured from a single subject. (a) Dependence of topological similarity (5) on time τ. (b) Evolution of brain functional connectivity within alpha and beta layers of considered network. Characteristic times $\tau_{1,2,3}$ corresponding to the presented brain graphs are indicated with arrows in lower plots.

3 Results of experimental EEG data analysis

Figure 3 illustrates the temporal evolution of reconstructed two-layer functional cortical network in alpha and beta frequency bands during the processing of a bistable visual stimulus. A curve in Figure 3a is a dependence of a topological similarity σ (5) on time. Figure 3b demonstrates the topologies of functional connectivity in alpha (upper row) and beta (lower row) frequency bands for different moments of time: $\tau_1 = 0.04$, $\tau_2 = 0.2$, $\tau_3 = 0.5$ s (these moments are shown in Fig. 3a by the arrows). The node size corresponds to the node degree (the number of links incident to the node). Illustration is based on the data of a single participant. At the same time, uncovered network behavior is typical and well-reproduced in a group of subjects and individual differences are only related with a slight variance of functional brain network topology.

At the moment of visual stimuli presentation (τ_1) the measure of similarity σ reaches 0.55 and the topology of functional connectivity in alpha and beta layers are quite different. Figure 3b shows that alpha layer demonstrates the poor involvement of occipito-parietal network (O and P EEG channels) which are associated with primary processing of visual information. The node corresponding to electrode O1 location is characterized by a high degree, due to a high number of large-scale links which couple frontal-temporal and occipito-parietal areas (O1–F4, O1–F8, O1–T4). The beta layer is characterized by a high degree of frontal nodes (Fp1 and Fp2), which have functional links with other frontal areas and with more remote somatosensory (Fp2–Cz, Fp2–C4) and parietal (Fp2–P4) areas.

When approaching the time moment τ_2, topology of functional connectivity has been changed in both alpha and beta layers. It is reflected in the measure of similarity σ reaching 0.65. One can see from Figure 3b, that large-scale links in alpha layer become less pronounced and node degrees are uniformly distributed across the network. The highest node degree is observed in somatosensory area which is caused by a functional connectivity between occipito-parietal and frontal areas through a Cz EEG channel. At the same time, the EEG channels in occipito-parietal area become highly connected on the beta layer having a pronounced hub at the Pz EEG channel. It indicates a strong involvement of the primary visual processing area into the perception of the visual stimuli. In both layers a somatosensory area (C3, Cz and C4 EEG channels) exhibits a large number of links and acts as a “bridge” between occipito-parietal and frontal areas.

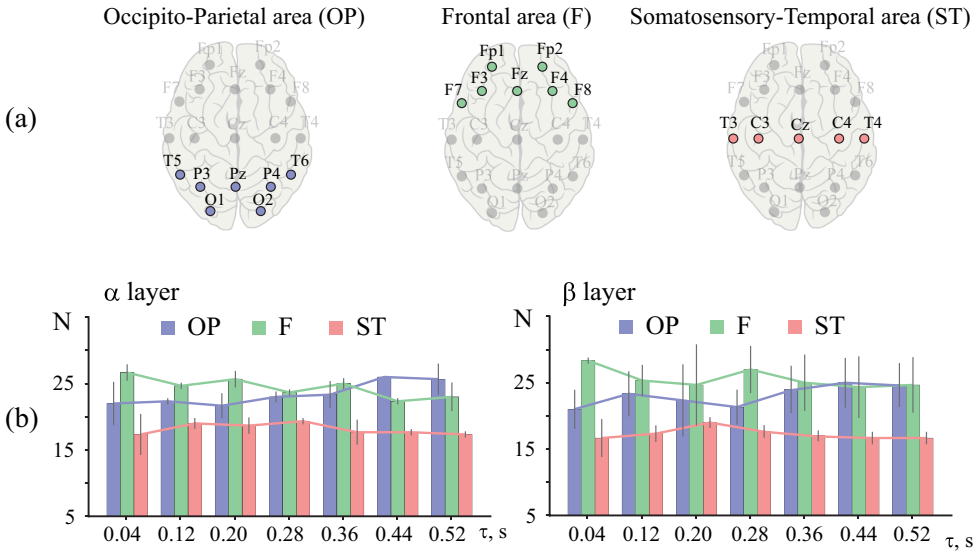

Fig. 4. (a) Considered brain areas: occipito-parietal area (OP), frontal area (F), somatosensory-temporal area (ST). (b) Histograms representing dynamics of total number, N, of links in OP (blue column), F (green column) and ST (red column) brain areas during the process of visual task performance collected over all participants in alpha (left panel) and beta (right panel) layers.

With the further increase of time in the sensory information processing up to τ_3, both alpha and beta layers demonstrate almost identical topology with $\sigma \approx 0.85$. One can conclude that during the process of visual stimuli perception multilayer functional cortical brain network is trying to fit an optimal structure providing an efficient use of cognitive brain resources to perform a certain visual task. Moreover, one can see that the frontal area, which is known to be associated with attention and decision-making [29], is not so actively engaged in visual stimuli processing compared to the occipito-parietal area in the final topology of brain functional connectivity. This may be due to the characteristics of the task assigned to the participants. The point is that visual stimuli were demonstrated for a very short time interval in order to capture the participant's first impression. Therefore, the participants of the experiment do not have enough time to fully focus on the visual stimulus, analyze it and make a decision on what he saw based on the provided analysis.

To compare the mechanisms of functional connectivity dynamics in a group of participants and find significant network properties we analyzed the evolution of characteristics, which reflect integral properties of multilayer functional brain network behavior. For such a characteristic we have considered the total number of links in different brain areas: occipito-parietal area (OP), frontal area (F) and somatosensory-temporal area (ST) (see Fig. 4a). For all 10 participants a significant increase in the link numbers in the OP area have been observed by the end of the visual stimuli demonstration in both alpha and beta layers ($p < 0.05$ via Wilcoxon test). On the contrary, the link number in the F area has decreased significantly in both layers as well ($p < 0.05$ via Wilcoxon test). At the same time, the number of links in the ST area did not perform significant changes ($p > 0.05$ via Wilcoxon test). Such behavior evidences the fact that during visual task performance functional network properties in separate layers evolve in a similar way. In particular, there is a tendency to activate occipito-parietal area and to decrease frontal area involvement. We can also conclude that somatosensory area is not significantly involved in visual perception task.

4 Conclusion

It is well-known that neural activity in alpha- and beta-bands is associated with the different types of perception. Changes in alpha-band activity are associated with the visual [30] or auditory attention [31] and variation of beta-waves energy – with the cognitive activity, related to the stimuli processing [32] and the shift of the brain to an attention state [33]. Role of the alpha/beta–band activity in the perceptual process is also reported in the context of the information transfer in the visual areas [8].

During visual information processing the beta-band activity plays the leading role [33]. For instance, beta–activity is associated with the excitation of neural ensembles, belonging to the "visual" area, located in the occipital lobe and the "attentional" area, located in the parietal lobe [34]. Alpha and beta oscillatory rhythms of the neural brain activity contribute to the neural communication between the different regions of the visual cortex [8,18].

In this paper we considered the evolution of the cortical network topology in alpha and beta frequency bands during visual sensory processing directed on capturing the first impression of participant. Two-layer cortical network was constructed via a pair-wise comparison of Fourier spectra of the corresponding EEG signals in specific frequency ranges, namely alpha (8–1 Hz) and beta (15–30 Hz) bands. Results obtained in this study lie in a course of modern theory of neural interactions standing behind the sensory processing performed in brain cortical network. Together with well-known mechanisms of stimulus-related brain activity in the occipito-parietal area we demonstrated an important role of the alpha and beta-band brain activity in a distributed cortical network. Having analyzed the evolution of layer's topology in time, we revealed the typical mechanisms of the cortical network cooperative reconfiguration during visual stimuli processing. Despite the fact that alpha and beta activities are usually associated with different processes, neural interactions within these frequency bands evolve in a similar way. We uncovered that during sensory processing network topology in both layers' changes in time in a way to optimize neural interactions in cortical network. In particular, network evolution aims at the activation of neural interactions in the occipito-parietal area responsible for primary visual processing and decreases the involvement of frontal area. We show that the described properties of the multilayer cortical network topology, which determine mechanisms of neural interactions during visual information processing, strongly depend on visual task complexity. By contrast, they are not crucially affected by the orientation of the Necker cube image. This is due to the specificity of the visual task assigned to the participants, which is focused on capturing their first impression, but not the process of image interpretation or decision-making.

This work has been supported by the Russian Science Foundation (Grant 17-72-30003).

References

1. J.M. Shine, M. Breakspear, P.T. Bell, K.A. Ehgoetz Martens, R. Shine, O. Koyejo, O. Sporns, R.A. Poldrack, Nat. Neurosci. **22**, 289 (2019)
2. J.M. Shine, R.A. Poldrack, NeuroImage **180**, 396 (2018)
3. A. Avena-Koenigsberger, B. Misic, O. Sporns, Nat. Rev. Neurosci. **19**, 17 (2018)
4. V.V. Makarov, M.O. Zhuravlev, A.E. Runnova, P. Protasov, V.A. Maksimenko, N.S. Frolov, A.N. Pisarchik, A.E. Hramov, Phys. Rev. E **98**, 062413 (2018)
5. K. Finc, K. Bonna, M. Lewandowska, T. Wolak, J. Nikadon, J. Dreszer, W. Duch, S. Kühn, Human Brain Mapping **38**, 3659 (2017)
6. K. Hwang, J.M. Shine, M. D'esposito, Cereb. Cortex **29**, 802 (2018)

7. A. Shenhav, S. Musslick, F. Lieder, W. Kool, T.L. Griffiths, J.D. Cohen, M.M. Botvinick, Ann. Rev. Neurosci. **40**, 99 (2017)
8. G. Michalareas, J. Vezoli, S. Van Pelt, J.-M. Schoffelen, H. Kennedy, P. Fries, Neuron **89**, 384 (2016)
9. S. Lagarde, N. Roehri, I. Lambert, A. Trebuchon, A. McGonigal, R. Carron, D. Scavarda, M. Milh, F. Pizzo, B. Colombet, B. Giusiano, S. Medina Villalon, M. Guye, G. Bénar, F. Bartolomei, Brain **141**, 2966 (2018)
10. R. Vicente, M. Wibral, M. Lindner, G. Pipa, J. Comput. Neurosci. **30**, 45 (2011)
11. P. Fries, Neuron **88**, 220 (2015)
12. M. Le Van Quyen, J. Foucher, J.-P. Lachaux, E. Rodriguez, A. Lutz, J. Martinerie, F.J. Varela, J. Neurosci. Methods **111**, 83 (2001)
13. K. Schiecke, M. Wacker, F. Benninger, M. Feucht, L. Leistritz, H. Witte, IEEE Trans. Biomed. Eng. **62**, 1937 (2015)
14. V.A. Maksimenko, A. Lüttjohann, V.V. Makarov, M.V. Goremyko, A.A. Koronovskii, V. Nedaivozov, A.E. Runnova, G. van Luijtelaar, A.E. Hramov, S. Boccaletti, Phys. Rev. E **96**, 012316 (2017)
15. J.E. Lisman, O. Jensen, Neuron **77**, 1002 (2013)
16. V.A. Maksimenko, S. van Heukelum, V.V. Makarov, J. Kelderhuis, A. Lüttjohann, A.A. Koronovskii, A.E. Hramov, G. van Luijtelaar, Sci. Rep. **7**, 2487 (2017)
17. E.A. Buffalo, P. Fries, R. Landman, T.J. Buschman, R. Desimone, Proc. Natl. Acad. Sci. **108**, 11262 (2011)
18. V.A. Maksimenko, A.E. Runnova, N.S. Frolov, V.V. Makarov, V. Nedaivozov, A.A. Koronovskii, A. Pisarchik, A.E. Hramov, Phys. Rev. E **97**, 052405 (2018)
19. J. Aru, J. Aru, V. Priesemann, M. Wibral, L. Lana, G. Pipa, W. Singer, R. Vicente, Curr. Opin. Neurobiol. **31**, 51 (2015)
20. R.T. Canolty, E. Edwards, S.S. Dalal, M. Soltani, S.S. Nagarajan, H.E. Kirsch, M.S. Berger, N.M. Barbaro, R.T. Knight, Science **313**, 1626 (2006)
21. J.M. Palva, S. Palva, K. Kaila, J. Neurosci. **25**, 3962 (2005)
22. J.M. Buldú, M.A. Porter, Netw. Neurosci. **2**, 418 (2018)
23. M. De Domenico, S. Sasai, A. Arenas, Front. Neurosci. **10**, 326 (2016)
24. J. Kornmeier, M. Pfäffle, M. Bach, J. Vision **11**, 12 (2011)
25. V.A. Maksimenko, A.E. Hramov, V.V. Grubov, V.O. Nedaivozov, V.V. Makarov, A.N. Pisarchik, Nonlinear Dyn. **95**, 1923 (2019)
26. V.A. Maksimenko, A.E. Runnova, M.O. Zhuravlev, V.V. Makarov, V. Nedayvozov, V.V. Grubov, S.V. Pchelintceva, A.E. Hramov, A.N. Pisarchik, PloS one **12**, e0188700 (2017)
27. V.A. Maksimenko, A.E. Hramov, N.S. Frolov, A. Lüttjohann, V.O. Nedaivozov, V.V. Grubov, A.E. Runnova, V.V. Makarov, J. Kurths, A.N. Pisarchik, Front. Neurosci. **12**, 949 (2018)
28. R.H.S. Carpenter, Biocybern. Biomed. Eng. **32**, 49 (2012)
29. A.E. Hramov, N.S. Frolov, V.A. Maksimenko, V.V. Makarov, A.A. Koronovskii, J. Garcia-Prieto, L.F. Antón-Toro, F. Maestú, A.N. Pisarchik, Chaos Interdiscip. J. Nonlinear Sci. **28**, 033607 (2018)
30. P. Sauseng, W. Klimesch, W. Stadler, M. Schabus, M. Doppelmayr, S. Hanslmayr, W.R. Gruber, N. Birbaumer, Eur. J. Neurosci. **22**, 2917 (2005)
31. J.J. Foxe, A.C. Snyder, Front. Psychol. **2**, 154 (2011)
32. P. Sehatpour, S. Molholm, T.H. Schwartz, J.R. Mahoney, A.D. Mehta, D.C. Javitt, P.K. Stanton, J.J. Foxe, Proc. Natl. Acad. Sci. **105**, 4399 (2008)
33. M. Gola, M. Magnuski, I. Szumska, A. Wróbel, Int. J. Psychophysiol. **89**, 334 (2013)
34. H. Laufs, J.L. Holt, R. Elfont, M. Krams, J.S. Paul, K. Krakow, A. Kleinschmidt, NeuroImage **31**, 1408 (2006)